Analysis of spermatogenesis and fertility in adult mice with a hypomorphic mutation in the *Mtrr* gene

Georgina E.T. Blake[1,2], Jessica Hall[1], Grace E. Petkovic[1], Erica D. Watson[1,2,*]

[1]Department of Physiology, Development and Neuroscience, [2]Centre for Trophoblast Research, University of Cambridge, Cambridge, UK

*Corresponding author: E.D. Watson, Department of Physiology, Development and Neuroscience, University of Cambridge, Physiological Laboratory, Downing Street, Cambridge, CB2 3EG, UK. Email: edw23@cam.ac.uk

Short title: Abnormal folate metabolism and male fertility

Word Count: 5,132

Table of Contents Summary

Transgenerational epigenetic inheritance (TEI) is a non-conventional mode of inheritance likely resulting from the transmission of epigenetic factors between generations via the germline. The *Mtrr*^{gt} mouse line is a model of TEI and abnormal folate metabolism. Here, we show that *Mtrr*^{gt} mutants exhibit normal spermatogenesis and fertility. Therefore, we suggest that these parameters can be disregarded as confounders of the TEI mechanism in the *Mtrr*^{gt} model.

ABSTRACT

Recent research has focused on the significance of folate metabolism in male fertility. Knocking down the mouse gene *Mtrr* impedes the progression of folate and methionine metabolism and results in hyperhomocysteinemia, dysregulation of DNA methylation, and developmental phenotypes (e.g., neural tube, heart, placenta defects). The $Mtrr^{gt}$ mouse line is a model of transgenerational epigenetic inheritance (TEI), the hypothesized cause of which is the inheritance of a yet-to-be determined epigenetic factor via the germline. Here, we investigate $Mtrr^{gt/gt}$ testes and sperm function compared to control C57Bl/6J testes to explore potential defects that might confound our understanding of TEI in the $Mtrr^{gt}$ model. Histological analysis revealed that adult $Mtrr^{gt/gt}$ testes are more spherical in shape than C57Bl/6J testes, though serum testosterone levels were normal and spermatogenesis progressed in a typical manner. Sperm collected from the cauda epididymis revealed normal morphology, counts, and viability in $Mtrr^{gt/gt}$ males. Correspondingly, $Mtrr^{gt}$ sperm contributed to normal pregnancy rates. Similar parameters were assessed in $Mtrr^{+/+}$ and $Mtrr^{+/gt}$ males, which were normal compared to controls. Overall, our data shows that the $Mtrr^{gt}$ allele is unlikely to alter spermatogenesis or male fertility. Therefore, it is improbable that these factors confound the mechanistic study of TEI in $Mtrr^{gt}$ mice.

Keywords: One-carbon metabolism, folate metabolism, folic acid, testes

INTRODUCTION

The importance of defective uptake and metabolism of the vitamin folate on testes function and male fertility has been reported (Boxmeer *et al.* 2009; Singh and Jaiswal 2013). In men, infertility correlates with reduced serum folate concentrations compared to fertile individuals (Murphy *et al.* 2011). Furthermore, dietary folate deficiency in mice is associated with delayed onset of meiosis during spermatogenesis (Lambrot *et al.* 2013). Indeed, dietary supplementation with folic acid improves fertility in subfertile men (Wong *et al.* 2002; Ebisch *et al.* 2003), though the molecular mechanism of this recovery is unclear. In general, metabolism of folate is required for DNA synthesis and is intertwined with methionine metabolism to promote the transmission of one-carbon methyl groups required for cellular methylation (Jacob *et al.* 1998; Ghandour *et al.* 2002). Therefore, folate metabolism is likely important for cell proliferation and widespread epigenetic changes, including during spermatogenesis.

Spermatogenesis is a highly coordinated differentiation event that occurs in the seminiferous tubules of the adult testes and results in the formation of spermatozoa. For mature spermatozoa to form, a series of mitotic and meiotic divisions must occur. Spermatogonia undergo a mitotic division to self-renew and form a primary spermatocyte. These cells move apically towards the lumen of the seminiferous tubule as they meiotically divide to form haploid spermatids (Smith and Walker 2014). Spermatids will then cytodifferentiate to give rise to spermatozoa, which are released into the tubule lumen and eventually leave the testis for the epididymis where they become functionally mature (Smith and Walker 2014). Spermatogenesis occurs in waves along the length of the seminiferous tubule to allow for the continuous production of sperm. The process is supported by somatic cells including Leydig cells and Sertoli cells (Smith and Walker 2014). Defects in spermatogenesis likely leads to subfertility or infertility (Anawalt 2013).

Folate metabolism is important for cell function. During its metabolism, folate is

converted to 5-methyl-tetrahydrofolate (5-methyl-THF), the main circulating folate, by the enzyme methylenetetrahyofolate reductase (MTHFR) (Smith *et al.* 2006). From 5-methyl-THF, a methyl group is transferred by the enzyme methionine synthase (MTR, also known as MS) to homocysteine to form methionine (Shane and Stokstad 1985). Methionine is the precursor of S-adenosyl methionine (Ado-Met or SAM), which is the one-carbon methyl donor for all methylation reactions in the cell including the methylation of DNA, RNA, and proteins via methyltransferases (Wainfan *et al.* 1975; Jacob *et al.* 1998; Ghandour *et al.* 2002; Xu and Sinclair 2015). A key enzyme required for the progression of one-carbon metabolism is methionine synthase reductase (MTRR), which is responsible for the activation of MTR through the reductive methylation of its vitamin B12 cofactor (Yamada *et al.* 2006). Furthermore, the folate cycle is also important for the *de novo* synthesis of the nucleotide thymidine from deoxyuridine monophosphate (Bistulfi *et al.* 2010). Therefore, folate metabolism likely plays an important role in genetic and epigenetic stability of a cell.

Beyond modulation of dietary intake of folate, evidence that folate metabolism might be important for male fertility comes from mutations in genes that encode for metabolic enzymes. For example, in humans, the *MTHFR* C677T mutation and the *MTRR* A66G mutation have independently been associated with reduced male fertility (Bezold *et al.* 2001; A *et al.* 2007). However, other reports show contradictory findings including some populations that have normal fertility despite the *MTRR* A66G mutation (Montjean *et al.* 2011; Mfady *et al.* 2014; Ni *et al.* 2015). Similarly, *Mthfr* knockout mice have a testes phenotype, though the severity of the defect depends upon the genetic background of the mouse (Chan *et al.* 2010). For instance, male *Mthfr*$^{-/-}$ mice with a BALB/c genetic background have fewer proliferating germ cells in the early postnatal period and infertility in adulthood (Chan *et al.* 2010). In contrast, a milder testes phenotype including normal fertility despite reduced sperm counts and abnormal testes morphology is observed in *Mthfr*$^{-/-}$ C57Bl/6J mice (Chan *et al.* 2010).

While a role for MTRR in spermatogenesis has not yet been established in mice, we previously reported that a hypomorphic mutation in the mouse *Mtrr* gene ($Mtrr^{gt}$) reduced MTR activity (Elmore *et al.* 2007) and caused hyperhomocysteinemia, global DNA hypomethylation, and locus-specific dysregulation of DNA methylation associated with changes in gene expression (Padmanabhan *et al.* 2013). Notably, an $Mtrr^{gt}$ allele can initiate the transgenerational epigenetic inheritance (TEI) of congenital abnormalities (Padmanabhan *et al.* 2013). For instance, when either the maternal grandfather or grandmother (i.e., the F0 generation) is an $Mtrr^{+/gt}$ heterozygote, a wide spectrum and frequency of congenital abnormalities are detected for at least up to four wildtype generations (Padmanabhan *et al.* 2013). This effect persists even after the transfer of F2 blastocyst-stage embryos into a normal uterine environment (Padmanabhan *et al.* 2013). In general, the mechanism behind this type of non-conventional inheritance is not well understood but it is thought to be independent of the DNA base sequence and likely involves the inheritance of an epigenetic factor(s) (e.g., DNA methylation, histone modifications, RNA content, etc.) via the germline (Blake and Watson 2016).

The search for inherited epigenetic factors in the $Mtrr^{gt}$ mouse line and other models of TEI is on-going and is generally focused on paternal inheritance to avoid confounding maternal influences (e.g., the uterine environment). While the TEI phenomenon occurs via the maternal lineage in the $Mtrr^{gt}$ model, an F0 $Mtrr^{+/gt}$ male or female can initiate the effect in their wildtype daughters. Therefore, it is logical to assess TEI mechanisms in sperm from $Mtrr^{gt}$ males. However, given the previously identified relationship between the vitamin folate and male fertility, attention should be paid to whether $Mtrr^{gt}$ mice are able to produce mature and fully functional spermatozoa. Therefore, the goal of this study is to assess spermatogenesis and fertility in males from the $Mtrr^{gt}$ mouse line to rule these parameters out as potential factors contributing to the mechanism behind TEI.

MATERIALS AND METHODS

Mice

Mtrr^{gt} mice were originally generated via a gene-trap (gt) insertion as previously described (Elmore *et al.* 2007). *Mtrr*$^{gt/gt}$ mice were produced from *Mtrr*$^{gt/gt}$ intercrosses. *Mtrr*$^{+/+}$ and *Mtrr*$^{+/gt}$ mice were produced from *Mtrr*$^{+/gt}$ intercrosses. C57Bl/6J mice (The Jackson Laboratory) were used as controls throughout the analyses since the *Mtrr*^{gt} mutation was backcrossed into a C57Bl/6J background for at least 8 generations. Control C57Bl/6J mice were bred in house and separately from the *Mtrr*^{gt} mouse line. *Mtrr*$^{+/+}$, *Mtrr*$^{+/gt}$, and *Mtrr*$^{gt/gt}$ genotypes were distinguished by PCR genotyping as previously described (Padmanabhan *et al.* 2013). Mice were fed a normal chow diet (Rodent No. 3 breeding chow, Special Diet Services) *ad libitum* from weaning. This research was regulated under the Animals (Scientific Procedures) Act 1986 Amendment Regulations 2012 following ethical review by the University of Cambridge Animal Welfare and Ethical Review Body.

Tissue collection and histology

Mice were culled by cervical dislocation. Testes were removed from 16-20 week-old mice that were proven fertile by mating to a female mouse. Each testis was weighed at the time of dissection. One testis per individual was snap frozen in liquid nitrogen for molecular analysis and the other testis was processed for histology. For paraffin embedding, each testis was fixed in 4% paraformaldehyde in 1x phosphate buffered saline (PBS) overnight at 4°C then prepared for paraffin embedding using standard procedures. Each paraffin embedded testis was sectioned to 7 μm in the transverse orientation and stained either with haematoxylin and eosin (H & E) stains or with Periodic Acid-Schiff (PAS) stain (395B, Sigma-Aldrich) using standard practices. Histological sections were imaged with a Nanozoomer 2.0RS digital slide scanner (Hamamatsu Photonics UK Ltd) and processed

with NDP.view2 viewing software (U12388-01, Hamamatsu Photonics) and ImageJ (64-bit) software (NIH, Bethesda MD, USA).

Immunohistochemistry

Histological sections were de-waxed, rehydrated and washed in 1x PBS. Sections were incubated with 3% hydrogen peroxide in 1x PBS at room temperature (RT) to quench endogenous peroxidase activity. Antigen retrieval was performed using trypsin tablets (T7168, Sigma-Aldrich) for 10 minutes according to the manufacturer's instructions. Tissue sections were incubated with blocking serum (5% donkey serum [D9663, Sigma-Aldrich], 1% bovine serum albumin [05470, Sigma-Aldrich] in 1x PBS) for 1 hour at RT and then incubated with rabbit anti-MTRR (26994-1-AP, Proteintech Europe) diluted to 1:100 in blocking serum overnight at 4°C. After washing in 1x PBS, tissue sections were incubated with horseradish peroxidase-conjugated donkey anti-rabbit IgG (ab6802, Abcam) diluted to 1:300 in blocking serum for one hour at RT. The colorimetric reaction was conducted with DAB (3,3-diaminobenzidine) chromagen substrate (ab64238, Abcam) according to the manufacturer's instructions. Controls included histological sections of testes that were incubated in blocking serum without the primary antibody or the secondary antibody. Sections were counterstained with haematoxylin and coverslip-mounted using DPX Mountant (06522, Sigma-Aldrich).

Analysis of allometric growth

Allometric growth of testis size in relation to body weight was calculated as follows (Gayon 2000).

$$\log_e y = \log_e a + b \log_e x$$

where x = body weight, y = testis weight, b = allometric co-efficient, and $\log_e a$ = the intercept of the line on the y axis. When $b > 1$ (positive allometry), the tissue in question

has a higher growth rate than the body as a whole. When $b < 1$ (negative allometry), the tissue has a lower growth rate than the body as a whole.

Spermatogenic staging of seminiferous tubules

Spermatogenic staging was performed on PAS-stained histological sections of testes. Eight sections from three males per genotypic group were analysed. Staging of seminiferous tubules occurred by randomly selecting an area of consistent size per testis histological section that contained at least 40 tubule cross-sections for analysis. Stages were assigned as previously described in detail (Meistrich and Hess 2013). Briefly, stages I-VII were denoted by the presence of round and elongated spermatids and the development and migration of the acrosome over the nucleus. Stage VIII was characterized by the release of elongated spermatids into the seminiferous tubule lumen. Stages IX-XII were defined by the condensation of chromatin and nuclear shape change in spermatids. Stage XII was identified by characteristic meiotic figures in spermatocytes.

RNA extraction and quantitative reverse transcription PCR (RT-qPCR)

RNA was extracted from adult testes using TRI-reagent (9424, Sigma-Aldrich) as per the manufacturer's instructions with an additional RNA precipitation step in 4M LiCl at -20°C overnight. cDNA was synthesised using RevertAid H Minus reverse transcriptase (EP0451, Thermo Scientific) and random hexamer primers (SO142, Thermo Scientific) using 1 µg of RNA in a 20 µl reaction according to manufacturer's instructions. Control reactions lacking reverse transcriptase were also performed. Each primer was diluted to a final concentration of 200 nM. Primer sequences (5' to 3' direction) included: *Folr1*, forward [F]: GGCCCTGAGGACAATTTACA, reverse [R]: TCGGGGAACACTCATAGAGG (Kooistra *et al.* 2013); *Hprt*, [F]: CAGGCCAGACTTTGTTGGAT, [R]: TTGCGCTCATCTTAGGCTTT (Rameix-Welti *et al.* 2014); *Mthfr*, [F]: AGCTTGAAGCCACCTGGACTGTAT, [R]:

AGACTAGCGTTGCTGGGTTTCAGA (Uthus and Brown-Borg 2006); wildtype *Mtrr*, [F]: GGGAAATTTGGAGCTATGTGG, [R]: CAGATGAGTCAAGACCCCAGT (Padmanabhan *et al.* 2013); *Slc19a1*, [F]: GGGTGTGCTACGTGACCTTT; [R]: ACGGAACTGATCACGGACTT (Kooistra *et al.* 2013). RT-qPCR conditions were optimized using standard curve analysis. Melt curve analysis was used to confirm target specificity. PCR amplification was conducted using MESA Green qPCR MasterMix Plus for SYBR Assay (05-SY2X-03+WOU, Eurogentec Ltd.) on a DNA Engine Opticon2 thermocycler (BioRad). Transcript levels were normalized to the housekeeping genes *Hprt*. Relative cDNA expression levels were analysed as previously described (Livak and Schmittgen 2001). Experiments were performed in duplicate with four to eight biological replicates. No template controls were included in each experiment.

Testosterone Concentration

Peripheral blood was collected using a 26-gauge needle through direct cardiac puncture after cervical dislocation. Blood was allowed to clot for 30 minutes at RT before centrifugation (2000 g, 10 minutes, 4°C) to separate serum from the blood cells. Serum was stored at -80°C. Serum testosterone levels were assessed using a testosterone enzyme-linked immunosorbent assay (ELISA) kit (EIA-1559, DRG International). According to the manufacturer, the ELISA has a sensitivity of 0.083 ng/ml of testosterone, an intra-assay variation of 3.3%, and inter-assay variation of 6.7%.

Sperm Counts, Viability and Morphology

Spermatozoa were collected from the cauda epididymis of at least three 16-20 week old males per genotypic group. The cauda epididymides were weighed at the time of dissection. One cauda epididymis per male was minced using a 26-gauge needle in 1x PBS that was pre-warmed to 37°C and incubated for 15 minutes at 37°C to form a sperm

suspension. The sperm suspension was diluted (1:4) in 1x PBS (at RT) and then incubated at 60°C for one minute as previously described (Wang 2003). Spermatozoa were counted using a haemocytometer and counts were normalised to cauda epididymis weight as previously published (Wang 2003). Viability of at least 100 sperm per male was assessed using a supravital staining method as previously described (Golshan Iranpour and Rezazadeh Valojerdi 2013). Briefly, a drop of sperm was mixed with 1% eosin (Sigma-Aldrich) for 15 seconds. Then, a drop of 10% aqueous nigrosin (Sigma-Aldrich) was thoroughly mixed in and a smear was made for analysis. Sperm morphology (e.g., normal, headless, hookless, amorphous) was analysed in at least 100 sperm per male according to published criteria (Wyrobek *et al.* 1983).

Fertility Analysis

To examine fertility, each male mouse (N=53 C57Bl/6J mice, N=40 *Mtrr*$^{gt/gt}$ mice) was mated with a female mouse. The time taken for a copulatory plug to form was recorded. Whether coitus resulted in pregnancy was determined by one of two methods: i) uteri were dissected between 6.5-10.5 days after the plug was detected or ii) the presence of a litter 18-20 days after the plug was detected.

Statistical analyses

Statistical analysis was performed using GraphPad Prism software (version 7). Ordinary one-way ANOVA, with Dunnett's multiple comparisons test, was used to analyse RT-qPCR, testes/male weights, allometry, testosterone concentrations, sperm parameters, and histological data. Independent unpaired t-tests were used to analyse data of time taken for a copulatory plug to form. The proportion of coitus that resulted in pregnancy was analysed using logistic regression assuming binomial errors. $P<0.05$ was considered significant.

RESULTS

MTRR *is widely expressed in the mouse testis*

To explore whether MTRR might be involved in spermatogenesis, the spatial expression pattern of MTRR protein was assessed in mouse testes. We performed immunohistochemistry on histological sections of adult testes from C57Bl/6J males using an antibody against MTRR. As expected, MTRR protein was widely detected throughout the testis including in Leydig cells, Sertoli cells, and in all spermatogenic cell types (Fig. 1*a-d)*. Subcellularly, MTRR protein expression was detected in the nucleus and cytoplasm of most cells (Fig. 1*b*). MTRR protein is more widely expressed in C57Bl/6J testes compared to the MTHFR protein, the latter of which is heterogeneously expressed in spermatocytes and interstitial cells of the testes (Garner *et al.* 2013).

The $Mtrr^{gt}$ allele is hypomorphic, such that the scale of *Mtrr* knockdown in $Mtrr^{gt/gt}$ mice was shown to vary between tissue types including liver, uterus, brain, kidney, and heart (from 19%-35% of control levels) (Padmanabhan *et al.* 2013). Therefore, we aimed to determine the degree of testes-specific genetic knockdown by assessing wildtype *Mtrr* transcript levels in $Mtrr^{+/+}$, $Mtrr^{+/gt}$ and $Mtrr^{gt/gt}$ males compared to C57Bl/6J males. RT-qPCR analysis was performed using PCR primers that were designed downstream of the gene-trap insertion in the *Mtrr* locus (Padmanabhan *et al.* 2013). Wildtype *Mtrr* mRNA expression was significantly decreased in $Mtrr^{+/gt}$ and $Mtrr^{gt/gt}$ testes to 59% and 14% of C57Bl/6J levels, respectively ($P<0.0001$; Fig. 1*e*). $Mtrr^{+/+}$ testes expressed levels of *Mtrr* mRNA similar to C57Bl/6J controls (Fig. 1*e*). Therefore, this data indicates robust *Mtrr* knockdown in $Mtrr^{gt/gt}$ testes, a finding similar to other $Mtrr^{gt/gt}$ tissue types (Padmanabhan et al, 2013).

To establish whether the expression of other genes involved in folate uptake and metabolism was altered by the $Mtrr^{gt}$ allele in testis, we performed an RT-qPCR analysis. mRNA expression of *Folr1*, *Slc19a1*, and *Mthfr* genes was similar in C57Bl/6J, $Mtrr^{+/+}$,

Mtrr$^{+/gt}$, and *Mtrr*$^{gt/gt}$ testes (Fig. 1*f-h*). This data suggests that cells in *Mtrr*$^{+/gt}$ and *Mtrr*$^{gt/gt}$ testes are unlikely to compensate for *Mtrr* deficiency, at least at the transcriptional level.

The testes of Mtrr$^{gt/gt}$ *mice are more spherical than C57Bl/6J control testes*

To explore the effects of the *Mtrr*^{gt} mutation on male body weight, C57Bl/6J, *Mtrr*$^{+/+}$, *Mtrr*$^{+/gt}$ and *Mtrr*$^{gt/gt}$ male mice were weighed at 16-20 weeks of age. Interestingly, we observed that *Mtrr*$^{+/gt}$ male body weight was significantly higher than C57Bl/6J controls (P<0.0001; Fig. 2*a*). A similar effect was not observed in *Mtrr*$^{+/+}$ or *Mtrr*$^{gt/gt}$ males, which were within the normal weight range compared to controls (Fig. 2*a*). This data suggests that the *Mtrr*^{gt} allele might have different metabolic repercussions when in heterozygous or homozygous form.

Next, testes from males of each genotype were weighed before processing for histological analysis. The average testis weight of *Mtrr*$^{gt/gt}$ males was slightly lower compared to C57Bl/6J controls (P=0.0133; Fig. 2*b*). *Mtrr*$^{+/+}$ and *Mtrr*$^{+/gt}$ testes weights were within the normal range (Fig. 2*b*). To determine the allometric scaling of the testis size in relation to body size, we calculated the allometric coefficient (b) for each genotype (Gayon 2000). We observed that testes of C57Bl/6J males have negative allometric growth since b <1 (b =0.879; Fig 2*c*) indicating a slightly lower testis growth rate compared to the body as a whole. Similarly, the testes of all *Mtrr* genotypes also showed negative allometric growth (*Mtrr*$^{+/+}$: b =0.561; *Mtrr*$^{+/gt}$: b =0.026; *Mtrr*$^{gt/gt}$, b =0.922; Fig 2*c*). Though statistically similar to C57Bl/6J, *Mtrr*$^{gt/gt}$ testis and body weights were nearly isometric (when b is equal to 1) indicating proportionate growth. However, the allometric co-efficient of *Mtrr*$^{+/gt}$ testes was significant lower compared to C57Bl/6J controls (P=0.023) and nearly zero (b =0.026) suggesting that as the body weight of *Mtrr*$^{+/gt}$ males increases, testes size is unlikely to change. Body composition of *Mtrr*^{gt} males should be assessed to better understand holistic metabolic changes resulting from abnormal folate metabolism.

While testes weight appeared relatively consistent across genotypes, gross analysis of the testis morphology revealed that compared to the ovoid shape observed in C57Bl/6J control, *Mtrr*$^{+/+}$ and *Mtrr*$^{+/gt}$ testes, the *Mtrr*$^{gt/gt}$ testes appeared rounder and shorter, and therefore closer to a spheroid shape (Fig. 2*d,f*). This observation was supported by a shorter major axis in *Mtrr*$^{gt/gt}$ testes relative to C57Bl/6J controls (P=0.023; Fig. 2*d-h*). To assess seminiferous tubule convolution and density, we quantified the number of times the seminiferous tubules crossed the sectional plane per mm^2 of testes. Tubule density was statistically similar in *Mtrr*$^{+/+}$, *Mtrr*$^{+/gt}$ and *Mtrr*$^{gt/gt}$ versus C57Bl/6J males (Fig. 2*i*). Furthermore, the average cross-sectional area of each tubule was equivalent in C57Bl/6 control, *Mtrr*$^{+/+}$, *Mtrr*$^{+/gt}$ and *Mtrr*$^{gt/gt}$ testes (Fig. 2*j*). Additionally, the thicknesses of the tunica albuginea, which is fibrous connective tissue that encapsulates the testis, and the tubule epithelium were unaffected by *Mtrr* deficiency (Fig. 2*k-m*). Overall, *Mtrr*$^{gt/gt}$ homozygosity in mice alters testis shape, yet seminiferous tubule gross morphology and density appeared unaffected.

Testosterone levels and spermatogenesis are unaltered by the Mtrr^{gt} *allele*

Next, to determine whether the *Mtrr*^{gt} mutation alters spermatogenesis, we assessed Leydig cell function by measuring serum testosterone levels using the ELISA method. Leydig cells are somatic cells located in the interstitial space between seminiferous tubules and produce testosterone in the presence of luteinizing hormone to drive spermatogenesis (Vasta *et al.* 2006). Although variable (co-efficient of variation was 1.07 ng/mL), the average serum testosterone concentrations in *Mtrr*$^{+/+}$, *Mtrr*$^{+/gt}$, and *Mtrr*$^{gt/gt}$ males were statistically similar to C57Bl/6J males (Fig. 3*a*) indicating normal Leydig cell function. Next, we quantified the number of Sertoli cells, which are somatic cells within seminiferous tubules that provide the niche for spermatogenic stem cell development (Smith and Walker 2014). These cells were identified by their characteristic triangular nucleus and prominent

nucleoli in histological sections of testes. The average number of Sertoli cells per seminiferous tubule section was similar in C57Bl/6J, *Mtrr*$^{+/+}$, *Mtrr*$^{+/gt}$ and *Mtrr*$^{gt/gt}$ testes (Fig. 3*b*). Altogether, this data suggests that supporting cells of the testes might not be affected by the *Mtrr*^{gt} allele, though further analysis is required to more fully assess Sertoli cell function in this context.

To explore the effects of the *Mtrr*^{gt} mutation on spermatogenesis, seminiferous tubules in histological sections were staged to assess the progression of the waves of spermatogenesis, maturation of the germinal epithelium and acrosome formation (Carrell and Aston 2013). Overall, normal progression of spermatogenesis (from spermatogonium to elongated spermatid) was apparent in C57Bl/6J, *Mtrr*$^{+/+}$, *Mtrr*$^{+/gt}$, and *Mtrr*$^{gt/gt}$ seminiferous tubules (Fig. 3*c*-*d*). No significant differences in the relative proportions of each spermatogenic stage or overt morphology of spermatogenic cells were observed compared to controls (Fig. 3*c*-*d*). Therefore, spermatogenesis appears to progress in a normal manner along the seminiferous tubule in *Mtrr*$^{+/gt}$ and *Mtrr*$^{gt/gt}$ mice.

Mtrr$^{+/gt}$ *and* Mtrr$^{gt/gt}$ *males have normal fertility*

Despite normal spermatogenesis, it was unclear whether spermatozoa from *Mtrr*$^{gt/gt}$ males were capable of maturing and, ultimately, fertilizing an oocyte at a similar rate as controls. To address this, mature spermatozoa were isolated specifically from the cauda epididymis for analysis. Sperm counts were determined using a haemocytometer and calculated as the number of sperm per mg of cauda epididymis and were similar in C57Bl/6J, *Mtrr*$^{+/+}$, *Mtrr*$^{+/gt}$, and *Mtrr*$^{gt/gt}$ males ($P>0.15$; Fig. 4*a*). The eosin/nigrosin smear supravital staining method revealed comparable percentages of viable sperm were present in each genotype analysed (92.7 to 97.4% viable sperm; $P>0.94$; Fig. 4*b*). Furthermore, at least 90% of spermatozoa from C57Bl/6J, *Mtrr*$^{+/+}$, *Mtrr*$^{+/gt}$ and *Mtrr*$^{gt/gt}$ showed a normal hooked morphology (Fig. 4*c*), and the frequency of abnormal sperm morphologies including

hookless (~1%), headless (~2-5%), or amorphous (~5-6%) sperm was similarly low between genotypes (Fig. 4*c*). Altogether, these data support the finding that abnormal folate metabolism caused by the *Mtrr*^{gt} allele did not affect sperm number, viability, or morphology.

Lastly, to assess fertility in *Mtrr*$^{gt/gt}$ males, we retrospectively analysed the ability of C57Bl/6J and *Mtrr*$^{gt/gt}$ males to produce a copulatory plug. This was determined by assessing the timespan between the establishment of a mating pair and detection of the plug. We found that 100% of C57Bl/6J males (52/52 males) and 95.2% of *Mtrr*$^{gt/gt}$ males (40/42 males) produced a copulatory plug within six days of mating. *Mtrr*$^{gt/gt}$ male mice took an average of 2.7 ± 0.2 days to copulate with a female mouse, which was slightly but significantly longer than the 2.1 ± 0.2 days (P=0.03) for C57Bl/6J control males (Fig. 4*d*). Due to its retrospective nature, a caveat to this experiment is that the female genotype was not initially taken into account. *Mtrr*$^{gt/gt}$ males were more often mated to *Mtrr*$^{gt/gt}$ female, which might be a potential confounding factor when determining the plug rate. When only matings with C57Bl/6J or *Mtrr*$^{+/+}$ females were considered, there was no apparent difference in plug rate between C57Bl/6J and *Mtrr*$^{gt/gt}$ males (P=0.84, Fig 4*e*). Next, to determine whether *Mtrr*^{gt} sperm were able to fertilize oocytes, we retrospectively assessed the ability of *Mtrr*$^{gt/gt}$ males to generate pregnancies after a copulatory plug was detected. This was determined by the presence of implantation sites in the dissected uterus or by pups littered. Pregnancies were generated at a similar rate between C57Bl/6J males (98.1%, N=52) and *Mtrr*$^{gt/gt}$ males (87.5%, N=40; P=0.0726, logistic regression assuming binomial errors) (Fig. 4*f*) regardless of female *Mtrr* genotype. Therefore, male fertility is likely unaffected by *Mtrr*$^{gt/gt}$ homozygosity.

DISCUSSION

Here we show that even though MTRR protein is widely expressed throughout the adult mouse testis, knockdown of *Mtrr* in adult male mice (e.g., $Mtrr^{+/gt}$ and $Mtrr^{gt/gt}$ males) does not alter spermatogenesis, sperm count in the cauda epididymis, or male fertility. However, $Mtrr^{gt/gt}$ testes were more spheroid in shape compared to ovoid control testes, though this difference did not alter testosterone production, seminiferous tubule density or spermatozoa formation. Therefore, it is possible to eliminate these parameters as confounding mechanistic factors in the study of TEI in the $Mtrr^{gt}$ mouse line.

Our conclusions differ from the observations of others showing associations between dietary folate deficiency or defective folate metabolism and male subfertility. For instance, infertility in men correlates with reduced serum folate concentrations (Murphy *et al.* 2011) and can be improved by folic acid supplementation (Wong *et al.* 2002; Ebisch *et al.* 2003). As demonstrated by folate-deficient mice, male subfertility may be associated with delayed onset of meiosis during spermatogenesis (Lambrot *et al.* 2013). Similarly, mutations in the human and mouse *MTHFR* gene are associated with altered sperm counts or reduced male fertility (Chan *et al.* 2010). In contrast, we showed that $Mtrr^{gt/gt}$ males appear to have normal testes morphology, spermatogenesis and fertility. There are a few possible reasons behind this difference as follows.

Firstly, the $Mtrr^{gt}$ allele is a hypomorphic mutation since wildtype *Mtrr* transcript is present in $Mtrr^{gt/gt}$ homozygous tissues including the testis (this study; Elmore *et al.* 2007; Padmanabhan *et al.* 2013). Why this occurs in the absence of a wildtype *Mtrr* allele is unclear, though one hypothesis is that the gene-trap that causes the $Mtrr^{gt}$ mutation might be spliced out in some circumstances (Elmore et al., 2007; Padmanabhan et al., 2013). In $Mtrr^{gt/gt}$ testis, the level of wildtype *Mtrr* mRNA expression was lower than other $Mtrr^{gt/gt}$ tissue types (e.g., heart, uterus, brain, kidney, liver) (Padmanabhan *et al.* 2013). While more extensive *Mtrr* transcriptional knockdown might imply that the testis is at increased

metabolic risk, *Mtrr*$^{+/gt}$ and *Mtrr*$^{gt/gt}$ testes generated mature and fertile sperm. Furthermore, transcriptional compensation by other genes involved in folate transport and metabolism was not observed in *Mtrr*^{gt} testes. It is possible that MTRR protein is translationally up-regulated in *Mtrr*$^{gt/gt}$ testes to compensate for low *Mtrr* transcript levels. However, this is not the case in other *Mtrr*$^{gt/gt}$ organs, which display proportionately low *Mtrr* transcript and MTRR protein levels (Elmore *et al.* 2007). A complete knockout of the *Mtrr* gene might result in a severe male fertility phenotype. Alternatively, knocking out *Mtrr* in mouse may not be conducive to life, similar to *Mtr*$^{-/-}$ mice (Swanson *et al.* 2001).

Secondly, genetic background effects may provide another potential reason for the absence of a spermatogenesis phenotype in *Mtrr*$^{gt/gt}$ mice. For instance, the severity of the testis phenotype in *Mthfr*-deficient mice is dependent upon whether the mutation occurred in a C57Bl/6 or BALB/c genetic background (Chan *et al.* 2010). *Mthfr*$^{-/-}$ BALB/c mice display oligospermia and infertility (Kelly *et al.* 2005; Chan *et al.* 2010) whereas *Mthfr*$^{-/-}$ C57Bl/6 mice are fertile but have a low sperm count (Chan et al, 2010). The *Mtrr*^{gt} mutation was backcrossed for at least eight generations into a C57Bl/6J genetic background (Padmanabhan *et al.* 2013). Since the *Mtrr*^{gt} allele has not been bred into an alternative genetic background, the phenotypic implications of genetic background on *Mtrr*-deficiency are unclear. However, evidence in humans supports genetic background effect since the *MTRR* A66G mutation in one population was shown to lead to reduced male fertility (Lee *et al.* 2006) whereas male fertility was not affected in other populations with the *MTRR* A66G mutation (Montjean *et al.* 2011; Mfady *et al.* 2014; Ni *et al.* 2015). How differences in genomic sequence outside of *MTRR* mutation influence metabolic and phenotypic severity should be explored further.

Lastly, it is possible that sperm are protected against the metabolic insult of *Mtrr* deficiency similar to cases of maternal folate deficiency when folate concentrations are normalised in fetal blood to maintain normal fetal growth (Ek 1980). Indeed, folate levels in

seminal plasma of men are greater than in blood plasma in normal dietary conditions (Wallock *et al.* 2001). Ado-Met levels vary between tissue types in the *Mtrr*$^{gt/gt}$ mice (Elmore *et al.* 2007), though this has not been correlated to the degree of tissue-specific *Mtrr* transcriptional knockdown. It will be necessary to measure folate and Ado-Met concentrations in *Mtrr*$^{gt/gt}$ testes and seminal fluid to test for a protective effect.

We also identified a novel dose-specific effect of the *Mtrr*^{gt} allele on male body weight. Compared to C57Bl/6J males, *Mtrr*$^{gt/gt}$ males displayed normal body weight whereas the body weight of *Mtrr*$^{+/gt}$ males was increased. This result implies that a single *Mtrr*^{gt} allele differentially affects one-carbon metabolism, and perhaps cellular metabolism in a broader sense compared to two *Mtrr*^{gt} alleles (Engin and Engin 2017). This is supported, in part, by the fact that *Mtrr*$^{+/gt}$ males have reduced plasma total homocysteine levels compared to C57Bl/6 control males, while *Mtrr*$^{gt/gt}$ males are hyperhomocysteinemic (Padmanabhan *et al.* 2013). It is unclear why the opposite metabolic effect occurs in *Mtrr*$^{+/gt}$ male mice compared to *Mtrr*$^{gt/gt}$ male mice, or how it relates to increased body weight particularly when obesity is more often associated with hyperhomocysteinemia (Amabile *et al.* 2016). Moreover, it appears that this body weight phenotype is late onset. *Mtrr*$^{+/gt}$ mice were assessed at 16-20 weeks of age (this study) and it was previously shown that *Mtrr*$^{+/gt}$ males display normal body weight from birth to at least 11 weeks of age (Elmore *et al.* 2007). However, the apparent lack of young *Mtrr*$^{+/gt}$ males with increased body weight might be attributed to the type of control used: Elmore et al. (2007) compared *Mtrr*$^{+/gt}$ male weights to *Mtrr*$^{+/+}$ male littermates whereas we used C57Bl/6J males as controls since ancestral *Mtrr* deficiency was shown to affect *Mtrr*$^{+/+}$ mice (Padmanabhan et al, 2013). Similar to Elmore et al. (2007), the current study showed no significant difference in body weight between *Mtrr*$^{+/+}$ and *Mtrr*$^{+/gt}$ males at 16-20 weeks. Why *Mtrr* haploinsufficiency alters body weight compared to C57Bl/6J controls is unclear and needs to be explored further.

Even though spermatogenesis and fertility were not affected by *Mtrr* deficiency, an abnormal spheroid shape characterized the $Mtrr^{gt/gt}$ testes. Since disruption of folate metabolism leads to altered nucleotide pools (Bistulfi *et al.* 2010) and hypomethylation of cell substrates (Wasson *et al.* 2006; Waterland *et al.* 2006; Dobosy *et al.* 2008), diminished cell proliferation may account for the abnormal shape. Though not well understood, determination of testes size likely occurs during highly proliferative phases of development (Sharpe 2006; Svingen and Koopman 2013). A shortened urogenital field caused by reduced proliferation during embryonic development might lead to a shortened, or rounder, testis shape (Wainwright *et al.* 2014). Investigating the effects of $Mtrr^{gt/gt}$ homozygosity on testis development in fetuses might help to explore the mechanism behind the spheroid testes phenotype.

The absence of a major testes phenotype in $Mtrr^{+/gt}$ and $Mtrr^{gt/gt}$ mice does not exclude the possibility of broad epigenomic differences in their sperm. Consistent with this hypothesis are fertile folate-deficient C57Bl/6 males with sperm that have altered epigenomes and with an increased risk of congenital malformations in their offspring (Lambrot *et al.* 2013). The epigenetic status of sperm is likely important in the context of intergenerational inheritance (Blake and Watson 2016). In general, somatic cells within the $Mtrr^{gt}$ mouse model display epigenetic instability (Padmanabhan et al, 2013), which might also extend to spermatozoa. We previously showed that $Mtrr^{+/gt}$ heterozygosity in male mice causes a transgenerational effect on development of their wildtype grandprogeny up to at least the F4 generation (Padmanabhan *et al.* 2013), though the mechanism behind TEI is unclear. Our current study shows that spermatogenesis and fertility are normal in $Mtrr^{gt}$ males making it possible to exclude these parameters as confounding mechanistic factors involved in the transgenerational inheritance.

DECLARATION OF INTEREST

The authors declare no conflicts of interest.

ACKNOWLEDGEMENTS

We thank Prof A. Ferguson-Smith for critical discussion of this manuscript. The work was funded by: a Wellcome Trust PhD studentship in Developmental Mechanisms (to G.E.T.B.) and a Lister Research Prize (to E.D.W.).

REFERENCES

A, Z.C., Yang, Y., Zhang, S.Z., Li, N., and Zhang, W. (2007) Single nucleotide polymorphism C677T in the methylenetetrahydrofolate reductase gene might be a genetic risk factor for infertility for Chinese men with azoospermia or severe oligozoospermia. *Asian J Androl* **9**(1), 57-62

Amabile, A., Migliara, A., Capasso, P., Biffi, M., Cittaro, D., Naldini, L., and Lombardo, A. (2016) Inheritable Silencing of Endogenous Genes by Hit-and-Run Targeted Epigenetic Editing. *Cell* **167**(1), 219-232

Anawalt, B.D. (2013) Approach to Male Infertility and Induction of Spermatogenesis. *J Clin Endocrinol Metab* **98**(9), 3532-42

Bezold, G., Lange, M., and Peter, R.U. (2001) Homozygous methylenetetrahydrofolate reductase C677T mutation and male infertility. *N Engl J Med* **344**(15), 1172-3

Bistulfi, G., Vandette, E., Matsui, S., and Smiraglia, D.J. (2010) Mild folate deficiency induces genetic and epigenetic instability and phenotype changes in prostate cancer cells. *BMC Biol* **8**, 6

Blake, G.E.T., and Watson, E.D. (2016) Unravelling the complex mechanisms of transgenerational epigenetic inheritance. *Curr Opin Chem Biol* **33**, 101-7

Boxmeer, J.C., Smit, M., Utomo, E., Romijn, J.C., Eijkemans, M.J.C., Lindemans, J., Laven, J.S.E., Macklon, N.S., Steegers, E.A.P., and Steegers-Theunissen, R.P.M. (2009)

511 Low folate in seminal plasma is associated with increased sperm DNA damage. *Fertil*
512 *Steril* **92**(2), 548-56
513
514 Chan, D., Cushnie, D.W., Neaga, O.R., Lawrance, A.K., Rozen, R., and Trasler, J.M.
515 (2010) Strain-specific defects in testicular development and sperm epigenetic patterns in
516 5,10-methylenetetrahydrofolate reductase-deficient mice. *Endocrinology* **151**(7), 3363-73
517
518 Dobosy, J.R., Fu, V.X., Desotelle, J.A., Srinivasan, R., Kenowski, M.L., Almassi, N.,
519 Weindruch, R., Svaren, J., and Jarrard, D.F. (2008) A methyl-deficient diet modifies
520 histone methylation and alters Igf2 and H19 repression in the prostate. *Prostate* **68**(11),
521 1187-95
522
523 Ebisch, I.M., van Heerde, W.L., Thomas, C.M., van der Put, N., Wong, W.Y., and
524 Steegers-Theunissen, R.P. (2003) C677T methylenetetrahydrofolate reductase
525 polymorphism interferes with the effects of folic acid and zinc sulfate on sperm
526 concentration. *Fertil Steril* **80**(5), 1190-4
527
528 Ek, J. (1980) Plasma and red cell folate values in newborn infants and their mothers in
529 relation to gestational age. *J Pediatrics* **97**(2), 288-92
530
531 Elmore, C.L., Wu, X., Leclerc, D., Watson, E.D., Bottiglieri, T., Krupenko, N.I., Krupenko,
532 S.A., Cross, J.C., Rozen, R., Gravel, R.A., and Matthews, R.G. (2007) Metabolic
533 derangement of methionine and folate metabolism in mice deficient in methionine
534 synthase reductase. *Mol Genet Metab* **91**(1), 85-97
535

536 Engin, A.B., and Engin, A. (2017) The Interactions Between Kynurenine, Folate,
537 Methionine and Pteridine Pathways in Obesity. *Adv Exp Med Biol* **960**, 511-27
538
539 Garner, J.L., Niles, K.M., McGraw, S., Yeh, J.R., Cushnie, D.W., Hermo, L., Nagano, M.C.,
540 and Trasler, J.M. (2013) Stability of DNA Methylation Patterns in Mouse Spermatogonia
541 Under Conditions of MTHFR Deficiency and Methionine Supplementation. *Biol Reprod*
542 **89**(5), 125
543
544 Gayon, J. (2000) History of the Concept of Allometry. *American Zoologist 40(5),* 748-58
545
546 Ghandour, H., Lin, B.-F., Choi, S.-W., Mason, J.B., and Selhub, J. (2002) Folate Status
547 and Age Affect the Accumulation of l-Isoaspartyl Residues in Rat Liver Proteins. *J Nutr*
548 **132**(6), 1357-60
549
550 Golshan Iranpour, F., and Rezazadeh Valojerdi, M. (2013) The epididymal sperm viability,
551 motility and DNA integrity in dead mice maintained at 4-6oC. *Iran J Reprod Med* **11**(3),
552 195-200
553
554 Jacob, R.A., Gretz, D.M., Taylor, P.C., James, S.J., Pogribny, I.P., Miller, B.J., Henning,
555 S.M., and Swendseid, M.E. (1998) Moderate folate depletion increases plasma
556 homocysteine and decreases lymphocyte DNA methylation in postmenopausal women. *J*
557 *Nutr* **128**(7), 1204-12
558
559 Kelly, T.L., Neaga, O.R., Schwahn, B.C., Rozen, R., and Trasler, J.M. (2005) Infertility in
560 5,10-methylenetetrahydrofolate reductase (MTHFR)-deficient male mice is partially
561 alleviated by lifetime dietary betaine supplementation. *Biol Reprod* **72**(3), 667-77

562

563 Kooistra, M., Trasler, J.M., and Baltz, J.M. (2013) Folate Transport in Mouse Cumulus-
564 Oocyte Complexes and Preimplantation Embryos. *Biol Reprod* **89**(3), 63, 1-9

565

566 Lambrot, R., Xu, C., Saint-Phar, S., Chountalos, G., Cohen, T., Paquet, M., Suderman, M.,
567 Hallett, M., and Kimmins, S. (2013) Low paternal dietary folate alters the mouse sperm
568 epigenome and is associated with negative pregnancy outcomes. *Nat Commun* **4**, 2889

569

570 Han-Chul, L., Yu-Mi, J., Sook, H.L., Kwang, Y.C., Seung-Hun, S., Nam, K.K., Kyo Won, L.,
571 Suman, L. (2006) Association study of four polymorphisms in three folate-related enzyme
572 genes with non-obstructive male infertility. *Hum Reprod* **21**(12), 3162-70

573

574 Livak, K.J., and Schmittgen, T.D. (2001) Analysis of relative gene expression data using
575 real-time quantitative PCR and the 2(-Delta Delta C(T)) Method. *Methods* **25**(4), 402-8

576

577 Meistrich, M.L., and Hess, R.A. (2013) Assessment of spermatogenesis through staging of
578 seminiferous tubules. In: 'Spermatogenesis. Methods in Molecular Biology (Methods and
579 Protocols)'. (Eds D. Carrell and K. Aston.) pp. 299-308. (Humana Press: Totowa, NJ.)

580

581 Mfady, D.S., Sadiq, M.F., Khabour, O.F., Fararjeh, A.S., Abu-Awad, A., and Khader, Y.
582 (2014) Associations of variants in MTHFR and MTRR genes with male infertility in the
583 Jordanian population. *Gene* **536**(1), 40-4

584

585 Montjean, D., Benkhalifa, M., Dessolle, L., Cohen-Bacrie, P., Belloc, S., Siffroi, J.P., Ravel,
586 C., Bashamboo, A., and McElreavey, K. (2011) Polymorphisms in MTHFR and MTRR

genes associated with blood plasma homocysteine concentration and sperm counts. *Fertil Steril* **95**(2), 635-40

Murphy, L.E., Mills, J.L., Molloy, A.M., Qian, C., Carter, T.C., Strevens, H., Wide-Swensson, D., Giwercman, A., and Levine, R.J. (2011) Folate and vitamin B(12) in idiopathic male infertility. *Asian J Androl* **13**(6), 856-61

Ni, W., Li, H., Wu, A., Zhang, P., Yang, H., Yang, X., Huang, X., and Jiang, L. (2015) Lack of association between genetic polymorphisms in three folate-related enzyme genes and male infertility in the Chinese population. *J Assist Reprod Genet* **32**(3), 369-74

Padmanabhan, N., Jia, D., Geary-Joo, C., Wu, X., Ferguson-Smith, A.C., Fung, E., Bieda, M.C., Snyder, F.F., Gravel, R.A., Cross, J.C., and Watson, E.D. (2013) Mutation in folate metabolism causes epigenetic instability and transgenerational effects on development. *Cell* **155**(1), 81-93

Rameix-Welti, M.A., Le Goffic, R., Herve, P.L., Sourimant, J., Remot, A., Riffault, S., Yu, Q., Galloux, M., Gault, E., and Eleouet, J.F. (2014) Visualizing the replication of respiratory syncytial virus in cells and in living mice. *Nat Commun* **5**, 5104

Shane, B., and Stokstad, E.L. (1985) Vitamin B12-folate interrelationships. *Annu Rev Nutr* **5**, 115-41

Sharpe, R.M. (2006) Perinatal Determinants of Adult Testis Size and Function. *J Clin Endocrinol Metab* **91**(7), 2503-5

613 Singh, K., and Jaiswal, D. (2013) One-carbon metabolism, spermatogenesis, and male
614 infertility. *Reprod Sci* **20**(6), 622-30
615
616 Smith, D.E., Kok, R.M., Teerlink, T., Jakobs, C., and Smulders, Y.M. (2006) Quantitative
617 determination of erythrocyte folate vitamer distribution by liquid chromatography-tandem
618 mass spectrometry. *Clin Chem Lab Med* **44**(4), 450-9
619
620 Smith, L.B., and Walker, W.H. (2014) The regulation of spermatogenesis by androgens.
621 *Semin Cell Dev Biol* **30**, 2-13
622
623 Svingen, T., and Koopman, P. (2013) Building the mammalian testis: origins,
624 differentiation, and assembly of the component cell populations. *Genes Dev* **27**(22), 2409-
625 26
626
627 Swanson, D.A., Liu, M.L., Baker, P.J., Garrett, L., Stitzel, M., Wu, J., Harris, M., Banerjee,
628 R., Shane, B., and Brody, L.C. (2001) Targeted disruption of the methionine synthase
629 gene in mice. *Mol Cell Biol* **21**(4), 1058-65
630
631 Uthus, E.O., and Brown-Borg, H.M. (2006) Methionine flux to transsulfuration is enhanced
632 in the long living Ames dwarf mouse. *Mech Ageing Dev* **127**(5), 444-50
633
634 Vasta, V., Shimizu-Albergine, M., and Beavo, J.A. (2006) Modulation of Leydig cell
635 function by cyclic nucleotide phosphodiesterase 8A. *Proc Natl Acad Sci U S A* **103**(52),
636 19925-30
637

638 Wainfan, E., Moller, M.L., Maschio, F.A., and Balis, M.E. (1975) Ethionine-induced
639 changes in rat liver transfer RNA methylation. *Cancer Res* **35**(10), 2830-5
640
641 Wainwright, E.N., Svingen, T., Ng, E.T., Wicking, C., and Koopman, P. (2014) Primary cilia
642 function regulates the length of the embryonic trunk axis and urogenital field in mice. *Dev*
643 *Biol* **395**(2), 342-54
644
645 Wallock, L.M., Tamura, T., Mayr, C.A., Johnston, K.E., Ames, B.N., and Jacob, R.A.
646 (2001) Low seminal plasma folate concentrations are associated with low sperm density
647 and count in male smokers and nonsmokers. *Fertil Steril* **75**(2), 252-59
648
649 Wang, Y. (2003) Epididymal sperm count. *Curr Protoc Toxicol* **Chapter 16**, Unit16.6
650
651 Wasson, G.R., McGlynn, A.P., McNulty, H., O'Reilly, S.L., McKelvey-Martin, V.J., McKerr,
652 G., Strain, J.J., Scott, J., and Downes, C.S. (2006) Global DNA and p53 region-specific
653 hypomethylation in human colonic cells is induced by folate depletion and reversed by
654 folate supplementation. *J Nutr* **136**(11), 2748-53
655
656 Waterland, R.A., Dolinoy, D.C., Lin, J.R., Smith, C.A., Shi, X., and Tahiliani, K.G. (2006)
657 Maternal methyl supplements increase offspring DNA methylation at Axin Fused. *Genesis*
658 **44**(9), 401-6
659
660 Wong, W.Y., Merkus, H.M., Thomas, C.M., Menkveld, R., Zielhuis, G.A., and Steegers-
661 Theunissen, R.P. (2002) Effects of folic acid and zinc sulfate on male factor subfertility: a
662 double-blind, randomized, placebo-controlled trial. *Fertil Steril* **77**(3), 491-8
663

Wyrobek, A.J., Gordon, L.A., Burkhart, J.G., Francis, M.W., Kapp, R.W., Jr., Letz, G., Malling, H.V., Topham, J.C., and Whorton, M.D. (1983) An evaluation of the mouse sperm morphology test and other sperm tests in nonhuman mammals. A report of the U.S. Environmental Protection Agency Gene-Tox Program. *Mutat Res* **115**(1), 1-72

Xu, J., and Sinclair, K.D. (2015) One-carbon metabolism and epigenetic regulation of embryo development. *Reprod Fertil Dev* **27**(4), 667-76

Yamada, K., Gravel, R.A., Toraya, T., and Matthews, R.G. (2006) Human methionine synthase reductase is a molecular chaperone for human methionine synthase. *Proc Natl Acad Sci U S A* **103**(25), 9476-81

FIGURE LEGENDS

Fig. 1. MTRR protein is widely expressed in adult mouse testes.

(*a*-*b*) Representative histological section displaying a seminiferous tubule (stage VIII) from an adult C57Bl/6J testis that was immunostained with an antibody against MTRR (brown). Nuclei are purple. (*b*) Higher magnification of boxed region in (*a*). (*c*-*d*) A seminiferous tubule from an adult C57Bl/6J testis immunostained with the secondary antibody only (i.e., no primary antibody control). (*d*) Higher magnification of boxed region in (*c*). Lc, Leydig cell; St, Sertoli cell; Sp, spermatogonia; Sc, spermatocyte; Rs, round spermatid; Es, elongated spermatid. Scale bars: *(a, c)*, 50 µm; *(b, d)*, 10 µm. (*e*-*h*) Graphs showing relative mRNA expression of (e) *Mtrr* (wildtype transcript), (f) *Folr1*, (g) *Slc19a1*, and (h) *Mthfr* in testes from C57Bl/6J control (black circles), $Mtrr^{+/+}$ (dark grey circles), $Mtrr^{+/gt}$ (light grey circles), and $Mtrr^{gt/gt}$ (white circles) mice as determined via RT-qPCR analysis. Data is plotted as mean ± sd. N= 4-6 males per genotype. Data is presented as fold change relative to C57Bl/6J controls, which was normalized to 1. A one-way ANOVA statistical test was performed on each data set. ****P<0.0001.

Fig. 2. $Mtrr^{gt/gt}$ testes appear more spherical in shape but are otherwise morphologically normal.

(*a*-*b*) Graphs showing (*a*) male body weight and (*b*) testis weight (per mouse) for mice with the following genotypes: C57Bl/6J controls (black circles), $Mtrr^{+/+}$ (dark grey circles), $Mtrr^{+/gt}$ (light grey circles) and $Mtrr^{gt/gt}$ (white circles). Data is plotted as mean ± sd. N=20-64 males per genotype. (*c*) Data depicting allometric growth analysis of testis weight in relation to body weight for C57Bl/6J (black circles, allometric co-efficient [b]=0.879), $Mtrr^{+/+}$ (dark grey circles, b =0.561), $Mtrr^{+/gt}$ (light grey circles, b =0.026, P=0.023) and $Mtrr^{gt/gt}$ (white circles, b =0.922) males. (*d*) Representative histological sections of whole testes stained with haematoxylin and eosin. C57Bl/6J, $Mtrr^{+/+}$, $Mtrr^{+/gt}$ and $Mtrr^{gt/gt}$ testes are

shown. Scale bar: 1 mm. (*e*) Histological section of C57Bl/6 control testis illustrating the parameters measured in (*g- m*). Boxed region represents a region higher magnification as shown in inset. Dotted line, outline of seminiferous tubule; i, major axis of testes diameter; ii, minor axis of testes diameter; iii, seminiferous tubule area; iv, longest seminiferous tubule epithelium width; v, shortest seminiferous tubule epithelium width; ta, tunica abuginea. (*f*) Image of representative C57Bl/6J and $Mtrr^{gt/gt}$ testes demonstrating overall shape. Scale bar: 1 mm. *(g-m*) Data representing measurements of testes and seminiferous tubule morphology for C57Bl/6J (black circles), $Mtrr^{+/+}$ (dark grey circles), $Mtrr^{+/gt}$ (light grey circles) and $Mtrr^{gt/gt}$ (white circles) males. Data is shown as mean ± sd. N = 4-5 males per genotype. Each dot represents the mean measurement of ≥ 6 histological sections per male. Measurements included: (*g-h*) testis diameter along the (*g*) major axis and (*h*) minor axis, (*i*) seminiferous tubule cross-sectional density, (*j*) average seminiferous tubule cross-sectional area, (*k-l*) seminiferous tubule epithelial width determined at the (k) longest and (*l*) shortest axis, and (*m*) the thickness of the tunica albuginea that encapsulates the entire testis. Statistical tests: one-way ANOVA tests. *P<0.05, ****P<0.0001.

Fig. 3. $Mtrr^{gt}$ mutation does not affect testosterone levels or spermatogenesis. (*a*) Serum testosterone concentrations as determined by ELISA in C57Bl/6J (black circles), $Mtrr^{+/+}$ (dark grey circles), $Mtrr^{+/gt}$ (light grey circles) and $Mtrr^{gt/gt}$ (white circles) males (N=7-8 males per genotype, except for $Mtrr^{+/+}$ group where N = 2 males). Data is represented as mean ± sd. (*b*) Graph depicting the average number of Sertoli cells per cross-section of seminiferous tubule within C57Bl/6J (black circles), $Mtrr^{+/+}$ (dark grey circles), $Mtrr^{+/gt}$ (light grey circles) and $Mtrr^{gt/gt}$ (white circles) testes. Data is plotted as mean ± sd. N = 5 males per genotype. At least three testis sections were assessed per male. (*c*) The proportion of seminiferous tubule sections categorized as one of the twelve stages of spermatogenesis

(stage I-XII) in C57Bl/6J, *Mtrr*$^{+/+}$, *Mtrr*$^{+/gt}$ and *Mtrr*$^{gt/gt}$ testes. N = 4 males per genotype. Six histological sections equally spread across the testis were assessed per male and ~220 seminiferous tubules were staged per testis section. Statistical analyses for *a*-*c*: one-way ANOVA tests. (*d*) Representative images of seminiferous tubules at stage VIII (top panel) and stage XII (bottom panel) of spermatogenesis for each genotype are shown. Histological sections of testes were stained with PAS stain. Es, elongated spermatid; Rs, Round spermatid; mf, meiotic figures. Scale bars: 50 μm.

Fig. 4. Sperm count, sperm viability, and male fertility are normal in *Mtrr*$^{gt/gt}$ mice. (*a*) Data showing the average sperm count normalized to cauda epididymis weight. Sperm collected from C57Bl/6J (black circles), *Mtrr*$^{+/+}$ (dark grey circles), *Mtrr*$^{+/gt}$ (light grey circles) and *Mtrr*$^{gt/gt}$ (white circles) cauda epididymides were assessed. Data is plotted as mean ± sd. N=3-17 males per genotype. (*b*) Graph depicting the percentage of total sperm that was viable as determined in eosin/nigrosin smears. Data is plotted as mean ± sd for C57Bl/6J (black circles), *Mtrr*$^{+/+}$ (dark grey circles), *Mtrr*$^{+/gt}$ (light grey circles) and *Mtrr*$^{gt/gt}$ (black circles) males. N=3-8 males per genotype. (*c*) Data showing the proportion of sperm with normal morphology (white) or abnormal morphology including headless sperm (light grey), amorphous sperm (dark grey) or hookless sperm (black) in C57Bl/6J, *Mtrr*$^{+/+}$, *Mtrr*$^{+/gt}$ and *Mtrr*$^{gt/gt}$ males. N=3-8 males per genotype. (*d*-*e*) Graphs indicating a retrospective analysis of the number of days between the establishment of a mating pair and detection of the copulatory plug for C57Bl/6J and *Mtrr*$^{gt/gt}$ males. Data is presented as mean ± sd. (*d*) Males were paired with C57Bl/6, *Mtrr*$^{+/+}$, *Mtrr*$^{+/gt}$ or *Mtrr*$^{gt/gt}$ female mice. N = 42-52 males. (*e*) Matings whereby C57Bl/6J and *Mtrr*$^{gt/gt}$ males were breed with C57Bl/6 and *Mtrr*$^{+/+}$ females only. N=45 C57Bl/6J males, N = 6 *Mtrr*$^{gt/gt}$ males. (*f*) The percentage of copulatory plugs generated by C57Bl/6J or *Mtrr*$^{gt/gt}$ males that resulted in pregnancy. N=40-52 litters

were assessed. Statistical analyses: (*a*-*c*) one-way ANOVA tests, (*d*-*e*) unpaired independent t tests, (*f*) Logistic regression (binomial errors). *P<0.05.

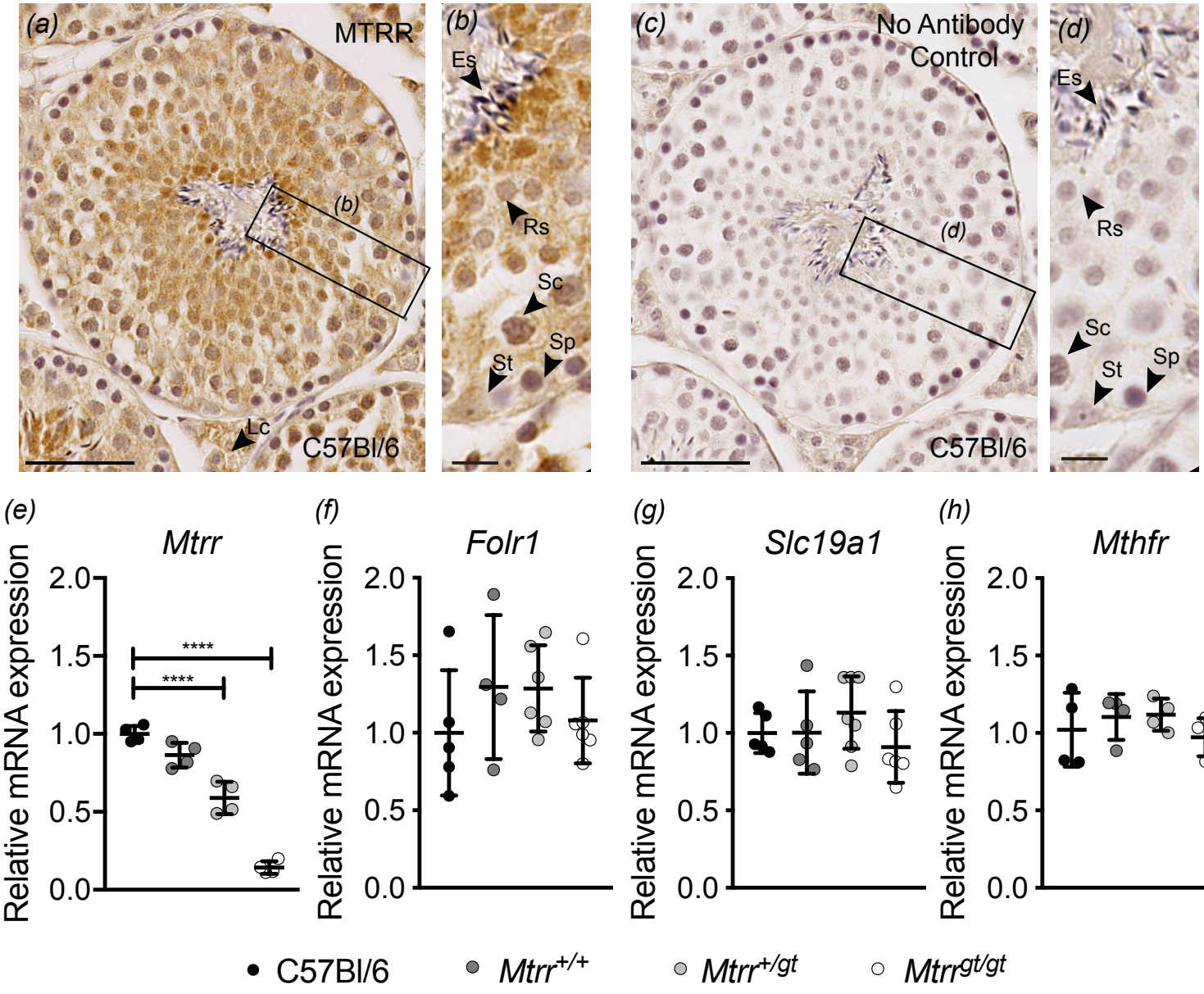
(a)
MTRR
(b)
Lc
C57Bl/6
(b)
Es
Rs
Sc
Sp
St
(c)
No Antibody Control
(d)
C57Bl/6
(d)
Es
Rs
Sc
Sp
St
(e)
Mtrr
Relative mRNA expression
2.0
1.5
1.0
0.5
0.0
****
****
(f)
Folr1
(g)
Slc19a1
(h)
Mthfr
C57Bl/6
Mtrr+/+
Mtrr+/gt
Mtrrgt/gt

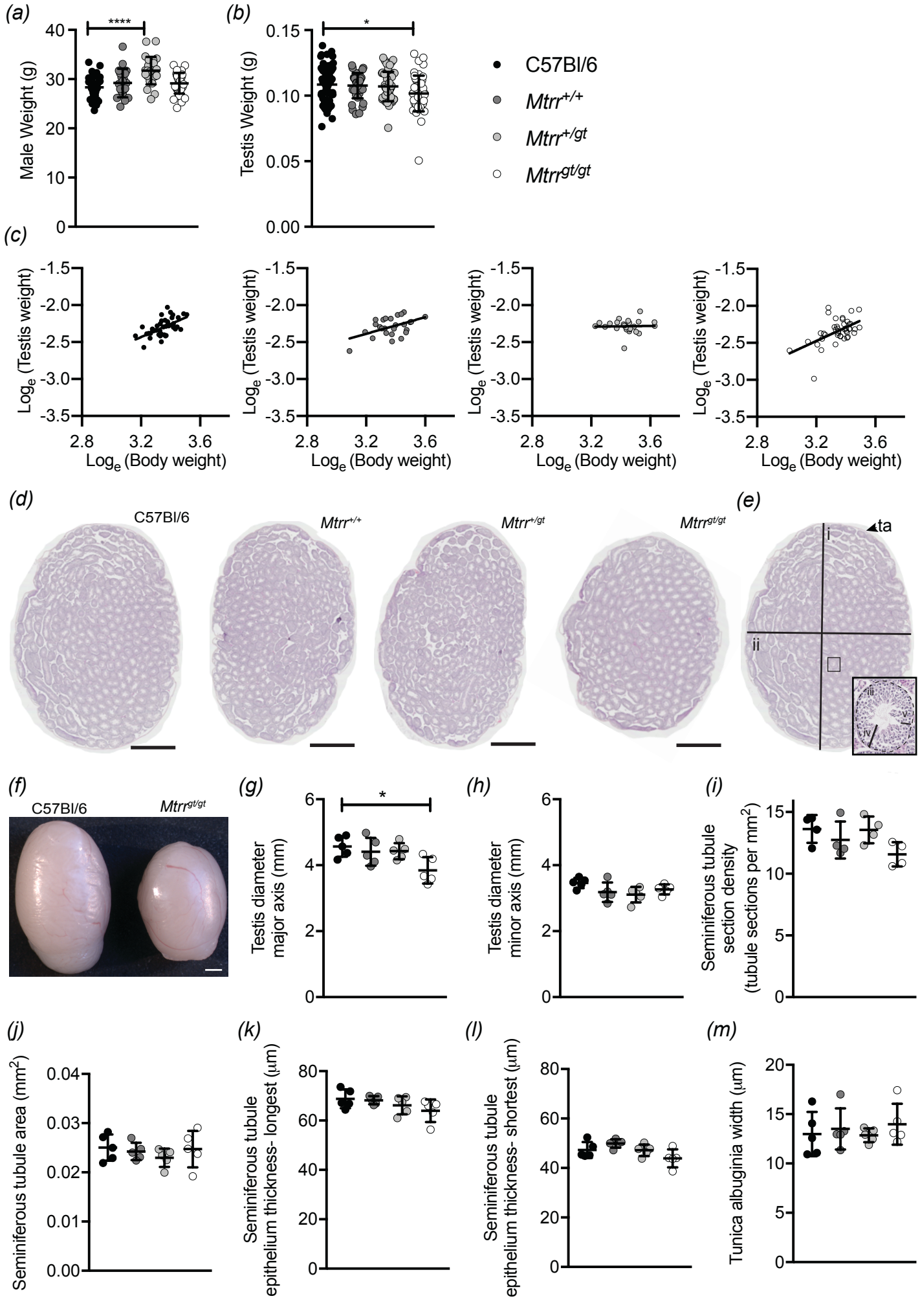
(a)
Male Weight (g)
****
(b)
Testis Weight (g)
*
C57Bl/6
Mtrr+/+
Mtrr+/gt
Mtrrgt/gt
(c)
Loge (Testis weight)
Loge (Body weight)
(d)
C57Bl/6
Mtrr+/+
Mtrr+/gt
Mtrrgt/gt
(e)
ta
i
ii
iii
iv
v
(f)
C57Bl/6
Mtrrgt/gt
(g)
Testis diameter major axis (mm)
(h)
Testis diameter minor axis (mm)
(i)
Seminiferous tubule section density (tubule sections per mm2)
(j)
Seminiferous tubule area (mm2)
(k)
Seminiferous tubule epithelium thickness- longest (µm)
(l)
Seminiferous tubule epithelium thickness- shortest (µm)
(m)
Tunica albuginia width (µm)

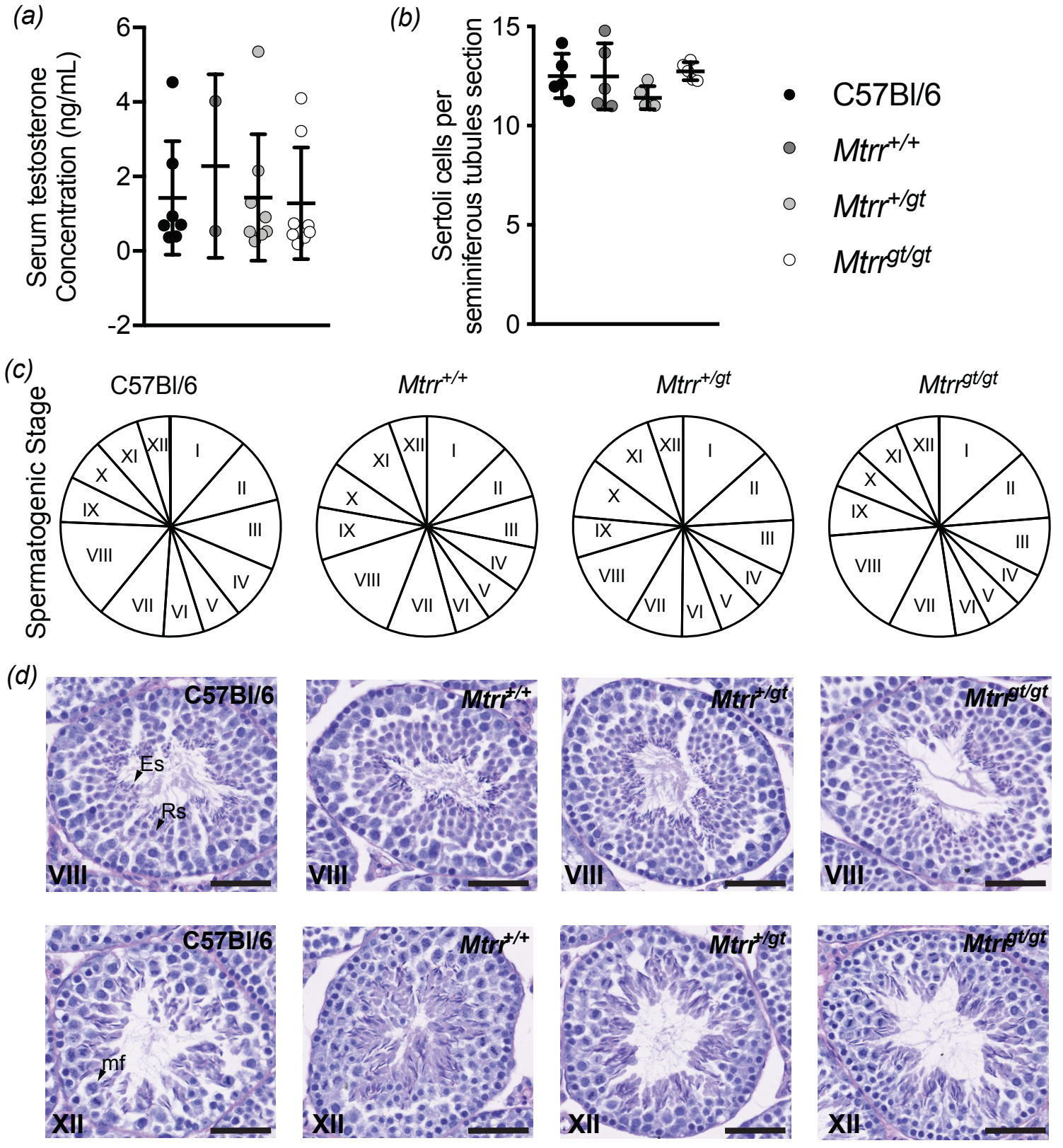
(a)
Serum testosterone Concentration (ng/mL)
6
4
2
0
-2
(b)
Sertoli cells per seminiferous tubules section
15
10
5
0
C57Bl/6
Mtrr+/+
Mtrr+/gt
Mtrrgt/gt
(c)
Spermatogenic Stage
C57Bl/6
Mtrr+/+
Mtrr+/gt
Mtrrgt/gt
I
II
III
IV
V
VI
VII
VIII
IX
X
XI
XII
(d)
C57Bl/6
Mtrr+/+
Mtrr+/gt
Mtrrgt/gt
Es
Rs
mf
VIII
XII

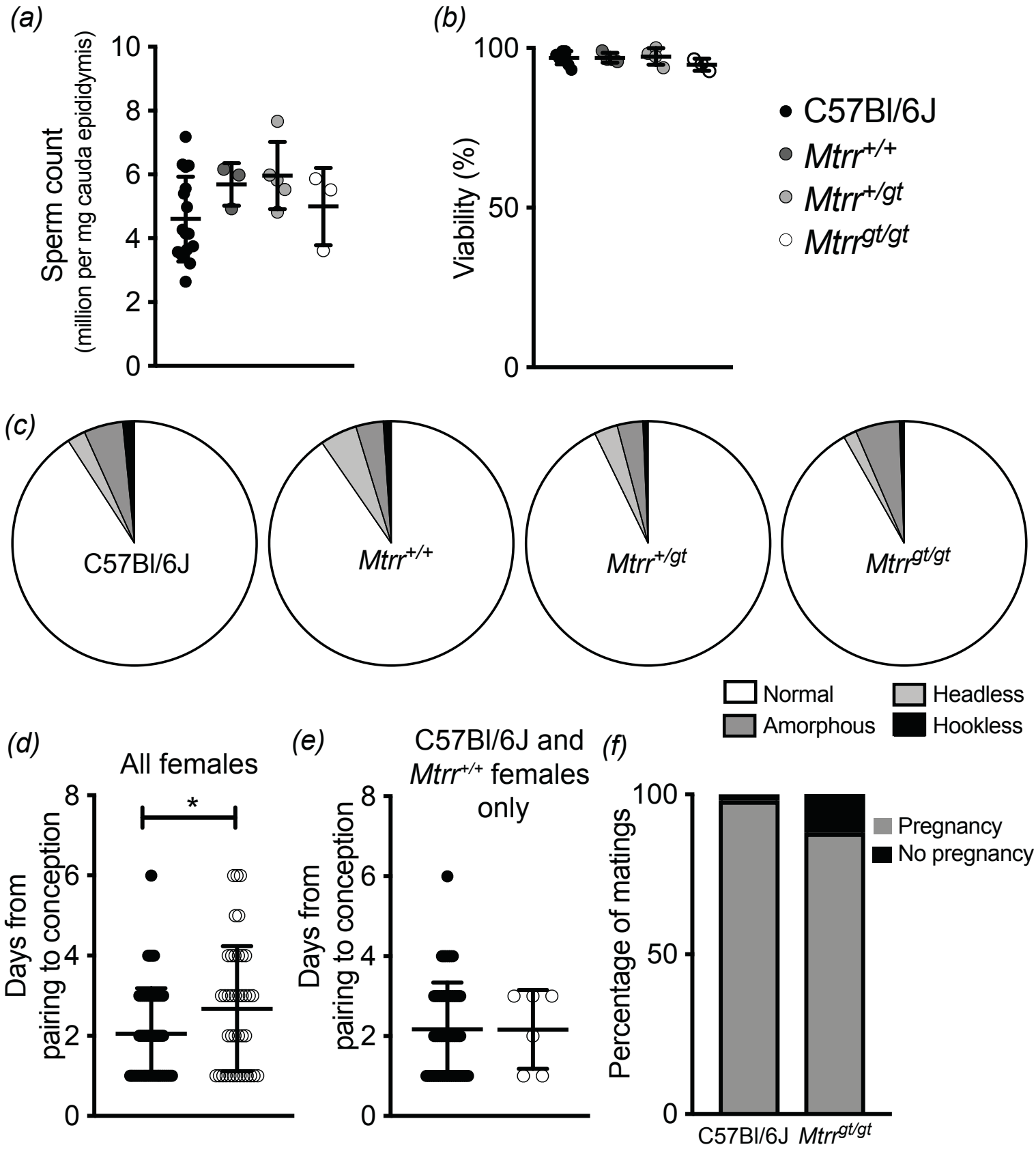
(a)
Sperm count
(million per mg cauda epididymis)
10
8
6
4
2
0
(b)
Viability (%)
100
50
0
C57Bl/6J
Mtrr+/+
Mtrr+/gt
Mtrrgt/gt
(c)
C57Bl/6J
Mtrr+/+
Mtrr+/gt
Mtrrgt/gt
Normal
Headless
Amorphous
Hookless
(d)
All females
*
Days from pairing to conception
8
6
4
2
0
(e)
C57Bl/6J and Mtrr+/+ females only
Days from pairing to conception
8
6
4
2
0
(f)
Percentage of matings
100
50
0
Pregnancy
No pregnancy
C57Bl/6J
Mtrrgt/gt